PSPICE MODEL FOR SIMULATING THE GIANT MAGNETOIMPEDANCE EFFECT IN MAGNETIC AMORPHOUS WIRES

Cristian Fosalau, Catalin Damian, Cristian Zeta

"Gh.Asachi" Technical University of Iasi, Faculty of Electrical Engineering, Bd. D.Mangeron 53, Iasi, 700050, Romania
(✉ cfosalau@ee.tuiasi.ro, +40 232 278 683, cdamian@ee.tuiasi.ro, czet@ee.tuiasi.ro)

Abstract

The paper presents an electrical model developed for Pspice simulation of the behavior of the magnetic amorphous wires (MAW) working under the Giant Magnetoimpedance (GMI) effect. The model was developed in order to facilitate the design of the signal conditioning circuitry belonging to the new category of transducers whose sensitive element is based on the GMI effect. The model is a complex one, owing to the fact that the effect is influenced by many internal or external factors, whose actions have to be taken into consideration. In the paper, an example on how the model can be applied to simulate a Colpitts oscillator is given next to its presentation and analysis.

Keywords: amorphous wire, giant magnetoimpedance effect, Pspice model, magnetic sensor.

1. Introduction

In the last decades, the magnetic materials have been developed in various forms and structures, so that they arrived to be employed in many applications and measurement devices. In particular, magnetic nanomaterials and those exhibiting amorphous structures have been proved to hold certain proprieties having as consequence interesting and useful effects that make them suitable to be employed in construction of sensitive devices. Such materials are magnetic amorphous wires with nearly zero magnetostrictivity, whose particular structure gives rise to the GMI effect [1,2]. This effect consists in sudden modification of the wire impedance whilst it is subject to a dc axial magnetic field polarization and also to a high frequency ac current flowing through it [2]. The effect can be explained in terms of circular magnetization variations of the wire with respect to some factors like external magnetic fields, axial and torsional stresses and ac current frequency and intensity. For relatively low frequency (usually up to 100 kHz), the impedance modification is caused by variation of the wire inductance caused by changes of the circular permeability into the wire shell. Above 100 kHz, the

skin effect occurs in the outer shell, it affecting both the resistive and inductive parts of the impedance. Overall, the GMI effect can be summarized in the following relation [3]

$$Z = R_{dc}kr\frac{J_0(k)}{2J_1(kr)}, \quad k = \frac{1+j}{\delta},$$ (1)

where R_{dc} is the wire resistance for *dc* current, J_0 and J_1 are Bessel functions, *r* is the wire radius and δ is the skin depth, which is given by the formula

$$\delta = \sqrt{\frac{2\rho}{\omega\mu_\Phi(H, i_{ac}, f, \xi, \sigma)}}.$$ (2)

The circular permeability, μ_ϕ, depends on the axial dc magnetic field, *H*, the *ac* current intensity and frequency, i_{ac} and *f*, the wire torsion, ζ, and the axial tensile stress, σ, while ρ is the wire resistivity. Explicitly, the complex impedance components can be assessed using the following equation

$$\underline{Z} = R + j\omega L = \frac{r}{2\sqrt{2\rho}}R_{dc}(1+j)\sqrt{\omega\mu_\Phi(H, i_{ac}, f, \xi, \sigma)}.$$ (3)

Based on the above effect, a large palette of sensors can be imagined. Several approaches have been already reported. Thus the MAWs can be used as sensitive elements to detect mechanical quantities such as: displacement, angle, force, strain, torsion, vibration or other quantities like electrical current and magnetic field [4-16].

In order to process the information carried in impedance variation with the measured quantity, several signal conditioning circuits have been reported. In [7,11,17] for example, the sensitive element is included into a Colpitts oscillator, whose oscillation amplitude and frequency depend on Z variation and finally on the input quantity. The circuit described in [18] is based on a voltage-controlled oscillator driven by the unbalanced voltage of a bridge containing the sensitive element. Its output supplies the bridge with an ac voltage whose frequency is dependent on the unbalance and hence on the Z variation. The performances obtained using these circuits have been assessed directly by measuring quantities resulting from the experimental model. In such cases, a lot of influence factors have been neglected since they could not been taken into consideration for practical reasons.

In the paper, we developed a Pspice model for emulating the wire electrical characteristics which helped us to design and simulate the sensors conditioning circuits in a more realistic manner, thus permitting to consider much more influence factors than in a real experiment.

The model implementation implies fulfilling the following steps:
– tracing the experimental characteristics
– finding the mathematical model by non-linear approximation of experimental curves

– obtaining the control signals materialized by voltages proportional to influence factors
– implementing the model in Pspice by using appropriate components
– assessing the model performances.

2. Experimental characteristics to be modeled

In our approach, we built the Pspice model for a nearly zero magnetostrictive amorphous wire having the composition $(Fe_{0.06}Co_{0.94})_7 2.5Si_{12.5}B_{15}$, the diameter of 0.122 mm and the length of 100 mm Owing to its exceptional sensitivity to axial magnetic fields, it has been employed to build a magnetic field sensor by mounting it into an operating scheme like that presented in Section 5 of this paper. The wire has been provided by the producer, the National Institute of Research & Development for Technical Physics Iaşi, Romania (www.phys-iasi.ro). However, the modeling procedure can be applied for any other magnetic material regardless of its composition or structure. For the sake of simplicity, we took into consideration only two influence factors upon the wire behaviour concerning the GMI effect: the axial magnetic field intensity, H, and the frequency of the ac current flowing through the wire, f. The model is based on a set of experimental data acquired using the setup presented in Fig.1.
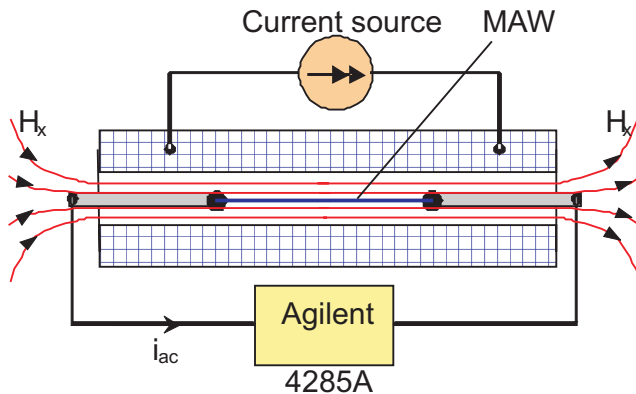

Fig. 1. Experimental setup for determining the wire characteristics.

The MAW is axially mounted into a coil fed by a constant *dc* current, which creates inside the magnetic field H, considered constant and uniform along the wire. The wire impedance components, L and R (considering the series model), are measured by using a precise LCR Meter, Agilent 4285A. All the parasitic influences of the connectors and leads have been compensated. The measurements were performed at the constant current i_{ac} = 10 mA. It has been proved that the influence of current i_{ac} upon the impedance variations is insignificant for values up to 25 mA [17].

In Fig. 2 and 3, the surfaces to be modeled acquired with the above experimental setup, $R(H, f)$ and $L(H, f)$ are presented; in Fig. 4 and 5, several sections in these surfaces representing the variations $L(H)$ and $L(f)$ are traced for H ranging between 0 and 30 Oe (0 and 2400 A/m) and f comprised between 100 kHz and 10 MHz.

These characteristics, along with the ones representing the $R(H)$ and $R(f)$ variations are the subjects of our Pspice modeling algorithm. Similarly, the method can be extended for modeling other influence factors like axial tensile stress, torsion or temperature.
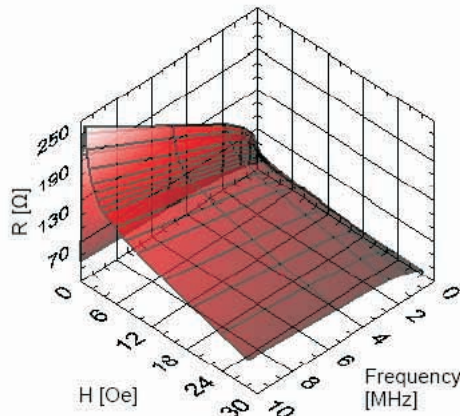

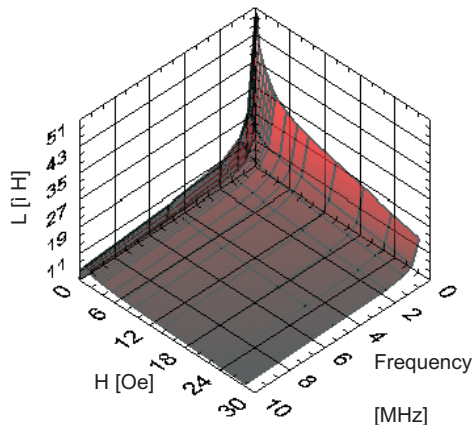Fig. 2. Representation of the experimental surface $R(H, f)$.

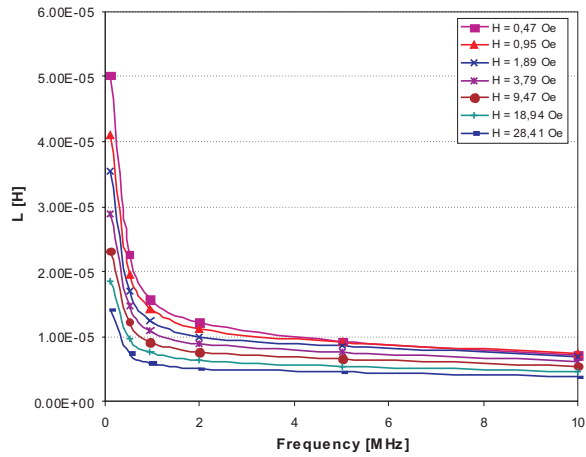Fig. 3. Representation of the experimental surface $L(H, f)$.
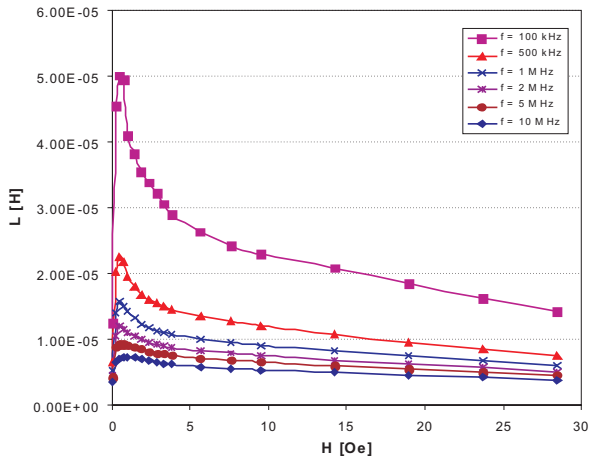
Fig. 4. *L(H)* for different values of *f*.

Fig. 5. *L(f)* for *H* variable.

3. Mathematical model

As can be observed from the above pictures, the dependencies are very nonlinear, meaning that the model might be a complex one. As stated earlier, we have to model two surfaces, $L(H, f)$ and $R(H, f)$. We found that the best fit for the two sets of characteristics is the power function. Hence, the two surfaces can be written as

$$L(f)\big|_{H_i} = a_{iL} f^{b_{iL}} \tag{4}$$

$$R(f)\big|_{H_i} = a_{iR} f^{b_{iR}} \tag{5}$$

By fitting the two curves, one obtains the coefficients a_{iL} and b_{iL} for modeling the inductance L, respectively a_{iR} and b_{iR} for resistance R. The values of these coefficients for several values of H are given in Table 1.

The goodness of fit is evaluated by calculating the parameters SSE (sum of square errors) and R^2. It was found that the worst fit was SSE = 2.3E-4 and R^2 = 0.99854 for H = 3.31 Oe.

The model is controlled by two quantities, H and f, implemented in the model as voltages. In the simulation process, H is an external parameter denoting the intensity of the field to be measured, which is modeled by an independent voltage source, V_H. As stated above, the model will be useful for simulating circuits that mostly have an oscillation as output. So, the common simulation for evaluating the circuit performances will be in the time domain (transient analysis in Pspice). In this case, f is seen as an internal control variable that will be materialized by a voltage proportional to the frequency of the current i_{ac}.

Supposing that the current is sinusoidal, its first derivative is proportional to frequency f

$$u(t) = U_{\max} \sin \omega t : \quad u'(t) = \frac{du(t)}{dt} = \omega U_{\max} \cos \omega t = 2\pi f U_{\max} \cos \omega t. \tag{6}$$

The amplitudes of $u(t)$ and $u'(t)$ are converted into two dc signals, U_1 and U_2 using peak detectors with diodes.

$$U_1 = U_{\max}, \qquad U_2 = 2\pi f U_{\max}. \tag{7}$$

Finally, the value of f is obtained by calculating the ratio

$$\frac{U_2}{2\pi U_1} = f. \tag{8}$$

Table 1.

H [Oe]	a_{iL}	b_{iL}	a_{iR}	b_{iR}
0.00E+00	5.99E-06	-3.02E-01	2.88E+01	1.72E-01
2.40E-01	1.53E-05	-4.68E-01	7.23E+01	4.18E-01
4.70E-01	1.71E-05	-4.64E-01	8.64E+01	4.08E-01
7.10E-01	1.66E-05	-4.69E-01	8.46E+01	4.35E-01
9.50E-01	1.54E-05	-4.18E-01	7.93E+01	4.07E-01
1.42E+00	1.46E-05	-4.10E-01	6.90E+01	4.04E-01
1.89E+00	1.37E-05	-4.02E-01	6.60E+01	3.77E-01
2.37E+00	1.31E-05	-4.00E-01	6.32E+01	3.67E-01
2.84E+00	1.27E-05	-3.95E-01	6.12E+01	3.55E-01
3.31E+00	1.23E-05	-3.87E-01	5.98E+01	3.49E-01
3.79E+00	1.19E-05	-3.77E-01	5.79E+01	3.47E-01
5.68E+00	1.11E-05	-3.67E-01	5.40E+01	3.42E-01
7.58E+00	1.06E-05	-3.51E-01	5.16E+01	3.29E-01
9.47E+00	1.01E-05	-3.48E-01	4.93E+01	3.19E-01
1.42E+01	9.15E-06	-3.45E-01	4.46E+01	3.00E-01
1.89E+01	8.28E-06	-3.36E-01	3.98E+01	2.80E-01
2.37E+01	7.47E-06	-3.22E-01	3.62E+01	2.49E-01
2.84E+01	6.67E-06	-3.12E-01	3.22E+01	2.13E-01

4. Pspice implementation

The frequency detector is represented in Fig. 6, while in Fig. 7 shows the full model of the wire. For simulating equation (5) of the detector we used the function d/dt from the ABM library of Pspice. Equation (7) is implemented with the EVALUE source E9. The voltage of 600 mV (over the sources E9 and E7) was added to U_1 and U_2 in order to compensate the average voltage drops on diodes.
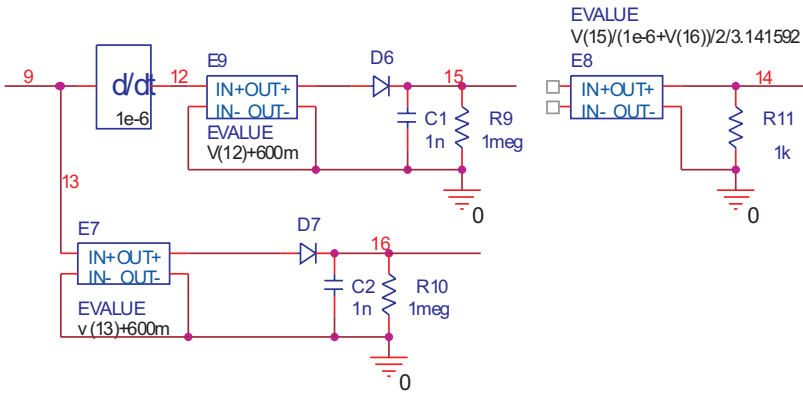
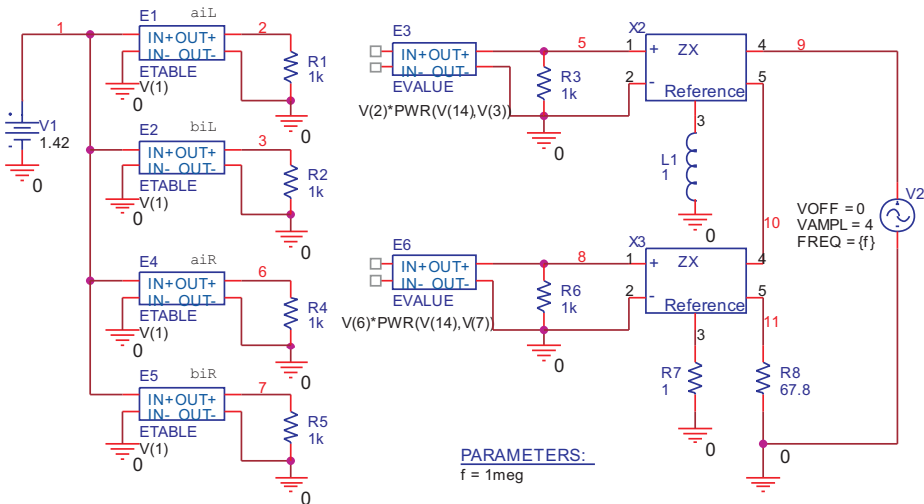Fig. 6. Pspice implementation of the frequency detector.

Fig. 7. Full model of the wire.

Referring to Fig. 7, the pairs of coefficients (H_i, a_{iL}), (H_i, b_{iL}), (H_i, a_{iR}) and (H_i, b_{iR}) are modeled with ETABLE sources E1, E2, E4 and E5, whilst EVALUE type sources E3 and E4 implement equations (3) and (4) . The inductance and resistance of the wire are modeled with voltage controlled impedances ZX, where L1 and R7 are reference devices having unitary values, being driven through signals applied between the pins 1 and 2.

vspace-0.3cm

5. Results and discussion

In order to assess the model goodness, we simulated its behaviour in a scheme similar to that used in the experimental setup. We traced the same sets of characteristics, by supplying the wire with a sinusoidal current of different frequencies comprised between 100 kHz and 10 MHz. In Fig. 8, the dependence of impedance *Z* with frequency, drawn in real conditions and by simulation for H = 3 Oe is presented. The maximum error in this case is 1.45 % at the frequency of 10 MHz.
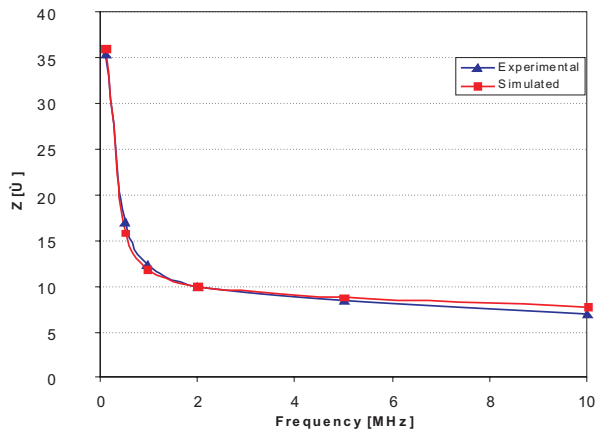
Fig. 8. Comparison between real and simulated results.

Another way to test the model efficiency was by including it in a Colpitts oscillator, which is the classical scheme used for conditioning the signal delivered by an application employing amorphous wires as sensitive elements (a magnetic field sensor for example) [17]. The same 100 mm long wire was mounted in an oscillator built according to Fig. 9.
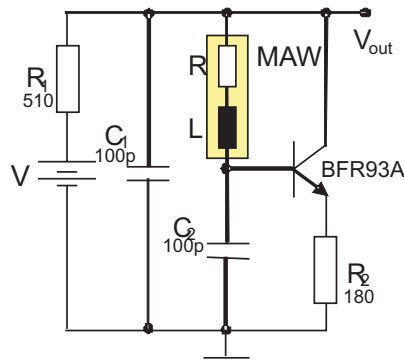
Fig. 9. The Colpitts oscillator scheme.

We measured its real free oscillating frequency, f_{real}, and we compared it with the frequency f_{sim}, obtained by simulating the operation of the same circuit. Several points have been chosen to cover mostly a nonlinear region. The results are presented in Table 2.

Table 2.

H [Oe]	f_{real} [MHz]	f_{sim} [MHz]	ε_f [%]
1.15	5.19	5.30	2.12
1.88	3.75	3.67	1.94
2.43	3.11	3.06	1.47
3.21	2.77	2.72	1.84
3.94	2.57	2.54	1.16
4.57	2.48	2.46	0.92
5.18	2.41	2.44	1.40
5.92	2.37	2.42	2.02

6. Conclusions

Analyzing the errors calculated in Table 1, we can conclude that the model is good enough for qualitative simulations, providing good accuracy even in nonlinear regions of the characteristic, where the mathematical approximation is quite imprecise. Theoretically, the model can be extended to any number of input quantities, but its complexity and computation time increase considerably. A drawback could be the fact that, due to rather important dispersion of wire characteristics, the model has to be updated when changing the sensor. By extension, the model presented in the paper might be successfully employed to simulate circuits devoted to process signals

delivered by sensors with sensitive elements based on any other nonlinear magnetic material.

Acknowledgements

References

[1] P.T. Squire, D. Atkinson, M.R. Gibbs: "Amorphous wires and their applications"". *J. of Magn. & Magn. Mat.*, 132, 1994, pp. 10–21.

[2] L.V. Panina, K. Mohri, T. Uchiyama, M. Noda: "Giant Magneto-Impedance in Co-Rich Amorphous Wires and Films". *IEEE Trans. Magn.*, vol. 31, 1995, pp. 1249–1260.

[3] K. Mohri et al: "Magneto-Impedance Element". *IEEE Trans. Magn.*, vol. 31, 1995, pp. 2455–2466.

[4] H. Chiriac, E. Hristoforou, M. Neagu, F. Borza: "Force measurements using Fe-rich amorphous wire as magnetostrictive delay line". *Sensors & Actuators*, vol. A91, June 2001, pp. 223–225.

[5] E. Hristoforou: "Magnetostrictive delay lines and their applications". *Sensors & Actuators A: Phys*, vol. 59, 1997, pp. 183–191.

[6] H. Chiriac, E. Hristoforou, M. Neagu, I. Darie, T.A. Ovari: "Amorphous wire delay lines used for magnetic field measurement". *IEEE Trans. Magn.*, vol. 33, 1997, pp. 4041–4043.

[7] K. Mohri, T. Kondo, H. Sugino: "Non-contact linear displacement sensors using amorphous-core multivibrators for mechanocardiography". *IEEE Trans. Magn.*, vol. MAG-21, Sept. 1985, pp. 2071–2073.

[8] L.P. Shen, K. Mohri: "Mechano-encephalogram based on amorphous wire micro SI aceeleration sensor". *IEEE Trans. Magn.*, vol. 37, July 2001, pp. 2007–2009.

[9] C. Fosalau, M. Cretu, O. Postolache: "A Circular Displacement Sensor Using Magnetostrictive Amorphous Wires". *IEEE Trans. Magn.*, vol. 36, May 2000, 557–560.

[10] L.P. Shen, K. Mohri, T. Uchiyama, Y. Honkura: "Sensitive acceleration sensor using amorphous wire SI element combined with CMOS IC multivibrator for environmental sensing". *IEEE Trans. Magn.*, vol. 36, Sept. 2000, pp. 3667–3669.

[11] K. Inada, K. Mohri, K. Inuzuka: "Quick Response Large Current Sensor Using Amorphous MI Element Resonant Multivibrator". *IEEE Trans. Magn.*, vol. 30, Nov. 1994, pp. 4623–4625.

[12] Y. Yoshida, A. Tayaoka: "Precise Current Sensor by means of Small-Angle Magnetization Rotation using Amorphous Wire and its Industrial Application". *IEEE Trans. Magn.*, vol. 29, Nov. 1993, pp. 3180–3182.

[13] V. Lemarquand: "Synthesis Study of Magnetic Torque Sensors". *IEEE Trans. Magn.*, vol. 35, Nov. 1999, pp. 4503–4510.

[14] K. Bushida, Mohri: "Sensitive micro-inductive effect in amorphous wires using high-pass filter and micro field sensor". *IEEE Trans. Magn.*, vol. 30, Nov. 1994, pp. 4626–4628.

[15] K. Bushida, K. Mohri, T. Kanno: "Amorphous wire MI micro magnetic sensor for gradient field detection". *IEEE Trans. Magn.*, vol. 32, Sept. 1996, pp. 4944–4946.

[16] C. Fosalau, M. Cretu, L. Nita: "A novel angle transducer using amorphous materials". *Mecatronica*, no. 2, 2004, pp. 34–37.

[17] C. Zet, C. Fosalau, E. Vremera: "A new magnetic field transducer based on magneto-impedance amorphous wires". *Buletinul Institutului Politehnic din Iasi (Bulletin of Polytechnic Institute of Iasi)*, tome LII, 2006, pp. 67-77.

[18] C. Fosalau, M. Temneanu, C. Donciu, C. Zet: "A low frequency current transducer with frequency output based on GMI effect in amorphous wires". *4th International Workshop on Amorphous and Nanostructured Magnetic Materials*, Iasi, August 29-31, 2007, pp. 34–39.